

## Spherical Tokamak Startup and Formation by ECH without Central Solenoid on LATE

H. Tanaka 1), T. Maekawa 1), M. Uchida 1), T. Yoshinaga 1), S. Nishi 1), J. Yamada 1), T. Matsumoto 1), T. Tanahashi 1), K. Yoshida 1), Y. Yamahana 1), Y. Matsumoto 1), W. Hamada 1), K. Komiya 1), A. Iwamae 2)

1) Graduate School of Energy Science, Kyoto University, Kyoto 606-8502, Japan

2) Graduate School of Technology, Kyoto University, Kyoto 606-8501, Japan

e-mail contact of main author: [h-tanaka@energy.kyoto-u.ac.jp](mailto:h-tanaka@energy.kyoto-u.ac.jp)

**Abstract.** Spherical tokamak startup and formation by ECH/ECCD without center solenoid is demonstrated and investigated on LATE. Spontaneous formation of initial closed flux surface occurs through a rapid current increase when a microwave is injected under a weak steady external vertical field  $B_v$  and at low gas pressure. After this current jump, plasma current increases by increasing  $B_v$  for equilibrium at larger plasma current. By injecting a 5GHz, 130 kW, 70 ms microwave pulse, plasma current is ramped up to 15 kA, which amounts to 16.7 % of the total toroidal coil current. The electric field at the current center is negative due to self-induction during the plasma current ramp. X-ray pulse height analysis shows the presence of high energy tail electrons with energy up to  $\sim 100$  keV. Plasma current may be carried by a uni-directional high energy electron tail, which may be generated and supported due to electron cyclotron harmonic heating by the mode-converted electron Bernstein wave with high refractive indices along the magnetic field.

### 1. Introduction

Removal of central solenoid (CS) from the fusion reactor based on Spherical Tokamak (ST) concept is essential and expected to reduce the construction cost greatly [1, 2]. Among startup scenarios without CS, use of electron cyclotron heating and current drive (ECH/ECCD) is promising because breakdown and current initiation can be fulfilled simultaneously and the required equipment for microwave power injection is only a small launcher remote from the plasma. Moreover, it is expected that ECH/ECCD occurs without density limit when the injected microwave is mode-converted to electron Bernstein wave (EBW). Then it is necessary to justify feasibility of this scheme by experiments.

The startup phase of a torus plasma is a dynamic process since it involves drastic changes of field topology, plasma production, confinement and equilibrium, which affect each other strongly. The theoretical research is very difficult because of its strong nonlinearity and unknown factors. The purpose of the LATE device is to demonstrate the startup of ST plasmas by ECH/ECCD without CS and to establish the physical bases. After the previous Fusion Energy Conference [3], we have augmented the microwave power and improved control system and power supplies for external vertical field  $B_v$ , and then, achieved significant progress in attained maximum plasma currents and understanding of startup physics.

### 2. Experimental Setup

Figure 1 shows the setup of the LATE device. The vacuum chamber of LATE is a cylinder with the diameter of 100 cm and the height of 100 cm. The outer diameter of the center post is 11.4 cm, enclosing 60 turns of Cu conductors for toroidal coil. There is no CS for inductive current drive. There are four sets of poloidal field coils, three are to generate vertical field  $B_v$

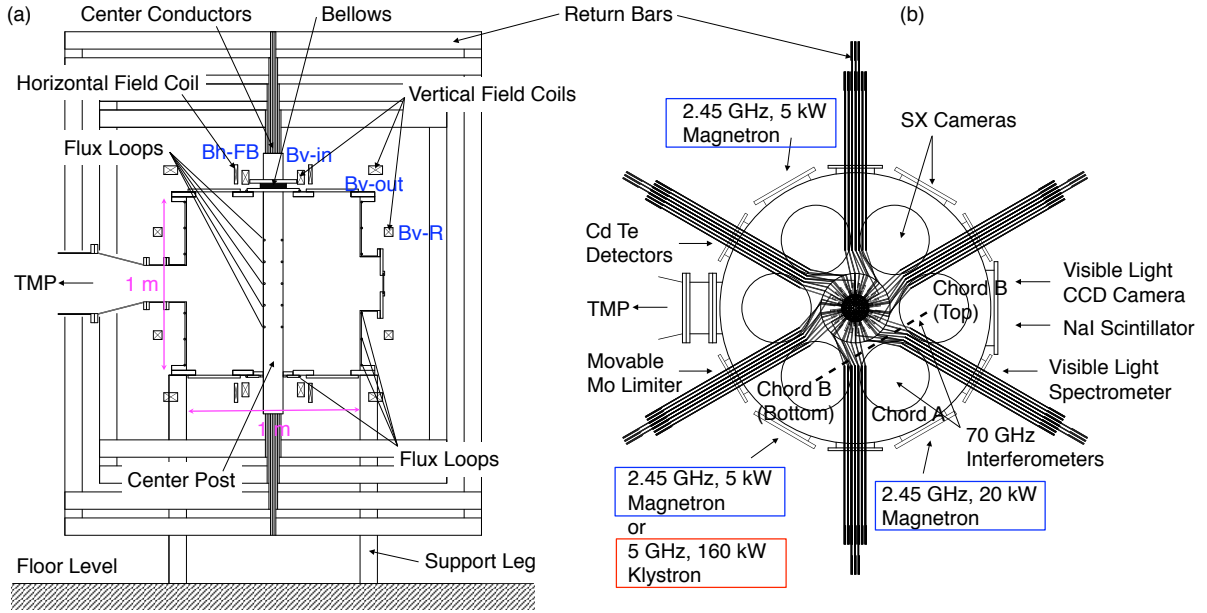


FIG. 1. The LATE device. (a) Side view. (b) Top view.

for equilibrium and one is to control the vertical position of the plasma. The vertical field coil currents are controlled by separate power supplies respectively with pre-programming. Then the vertical field decay index can be changed during a discharge to control the plasma shape. Three 2.45 GHz magnetrons ( $\leq 45$  kW in total,  $\leq 2$  sec) and a 5 GHz klystron ( $\leq 160$  kW,  $\leq 70$  ms) are used for ECH. All the microwaves are injected from radial ports with small injection angles (about 15 degree) from normal to the toroidal field, to aim the effective mode conversion to electron Bernstein wave (EBW) by the O-X-B process. An X-ray pulse height analysis system has been equipped. A CdTe detector is used to detect X-rays with energy from 20 to 200 keV, which are emitted forwardly by the electrons carrying the plasma current. The tangential radius of line-of-sight is  $R = 25$  cm and spacial resolution is about 5 cm.

### 3. Experimental Results and Discussion

Figure 2 shows a typical discharge with a 5 GHz microwave pulse (130 kW, 60 ms). The total toroidal coil current  $I_T$  flowing through the center post is 90 kA and the fundamental EC resonance layer locates at  $R = 10$  cm. Under a steady external vertical field ( $B_v = 56$  G at  $R = 25$  cm) with a low decay index ( $n = 0.08$  at  $R = 25$  cm) and at low hydrogen gas pressure ( $p_{H_2} \leq 1 \times 10^{-2}$  Pa), breakdown takes place at the fundamental EC resonance layer and a weak plasma current  $I_p$  appears. Then,  $I_p$  increases rapidly to 6 kA in about 6 ms, resulting in the spontaneous formation of closed flux surfaces. This current jump bridges the gap between the open field equilibrium maintained by a pressure-driven current and the closed field equilibrium at a larger current, and may be due to the efficient current generation by the asymmetric confinement of electrons along the field line appearing upon the transition of field topology [4]. After the current jump,  $I_p$  is increased by increasing  $B_v$  for equilibrium at larger plasma current, and reaches 12 kA at the end of the microwave pulse. The ramp-up rate of applied  $B_v$  is set to  $\sim 8$  G/10ms and  $I_p$  increases at nearly constant rate of  $\sim 1$  kA/10ms. Plasma current profiles and poloidal flux surfaces are reconstructed from flux loop signals with a current profile model [5]. The radial position of plasma current center,  $R_j$ , is between the 2nd and the 3rd

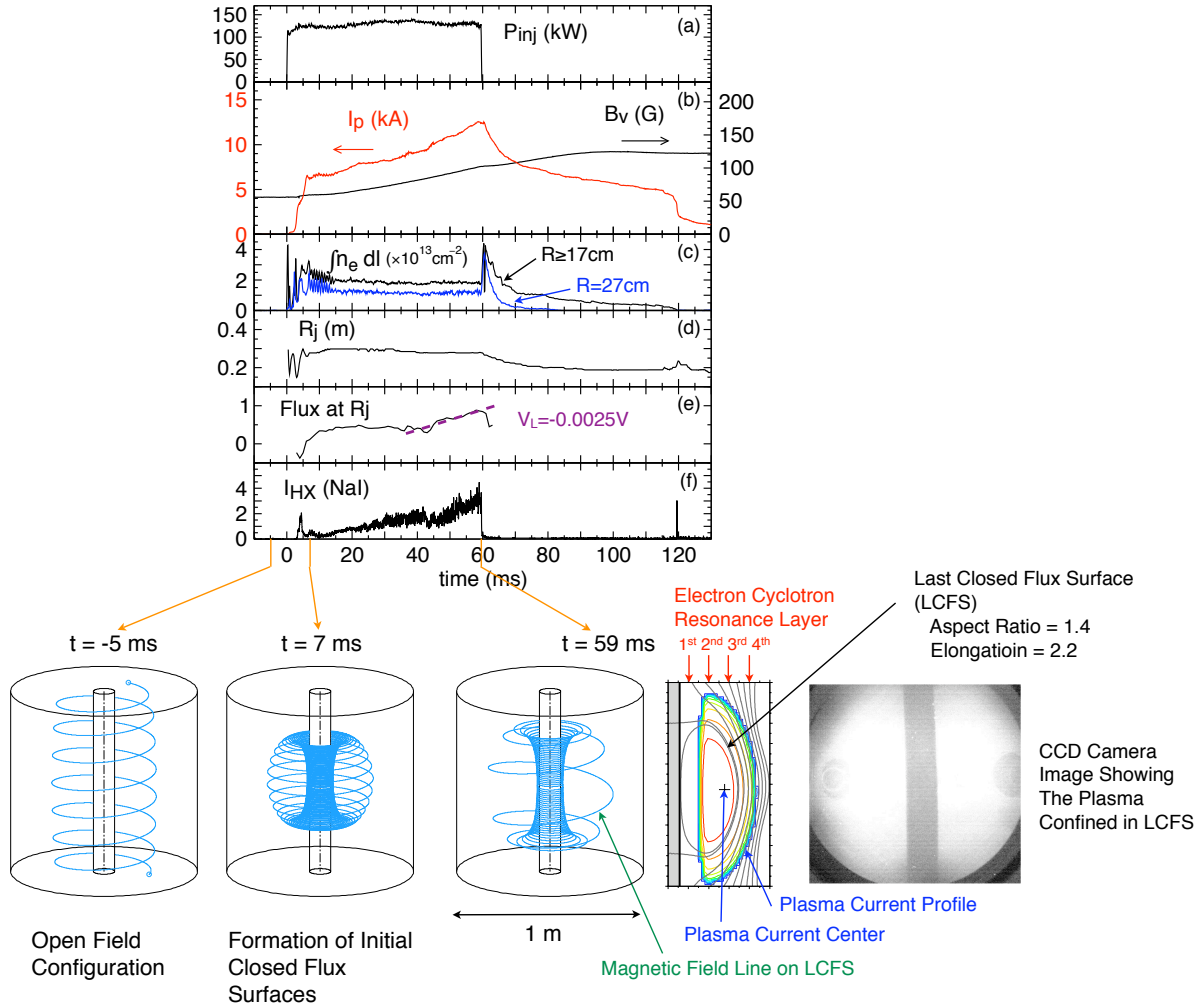


FIG. 2. Waveforms, field lines, current profile and CCD camera image for a  $I_p = 12$  kA discharge with 5 GHz microwave. (a) Injected microwave power; (b) Plasma current and applied vertical field at  $R = 25$  cm, (c) Line-integrated electron density; (d) Radial position of plasma current center; (e) Poloidal flux at the plasma current center; (f) Hard X-ray signal from NaI scintillator.

EC resonance layer. The current profile is vertically elongated and encompasses the EC harmonic resonance layers from the 2nd to the 4th. The last closed flux surface (LCFS) has an elongation of  $\kappa = 2.2$  and an aspect ratio of  $R/a = 20.0$  cm/ $14.3$  cm = 1.4, which is also seen in the plasma image taken by a CCD camera. The poloidal flux at the current center  $R_j$  is calculated and it is shown that the flux increases nearly at a constant rate from  $t = 45$  ms to  $t = 57$  ms, corresponding to negative one-turn loop voltage  $V_L = -0.025$  V. This negative loop voltage is produced by self-induction during the plasma current ramp. Hard X-ray emission measured by a NaI scintillator increases as  $I_p$  and  $B_v$  increase, suggesting that high energy tail electrons are produced and build-up. The final value of  $I_p$  amounts to 13.5 % of the total toroidal coil current  $I_T$  and the magnetic field line on LCFS has a large pitch angle and shows the characteristics of the ST configuration. The line averaged electron density is  $4 \times 10^{17}$  m $^{-3}$  and exceeds the plasma cutoff density. Figure 3 (a) shows the soft X-ray emission profile reconstructed from soft X-ray camera signals by the computer tomography (CT) method. The soft X-ray emission have maximum around the 2nd EC resonance layer. Above experimental evidences suggest that the injected microwave is mode-converted to EBW and then absorbed at

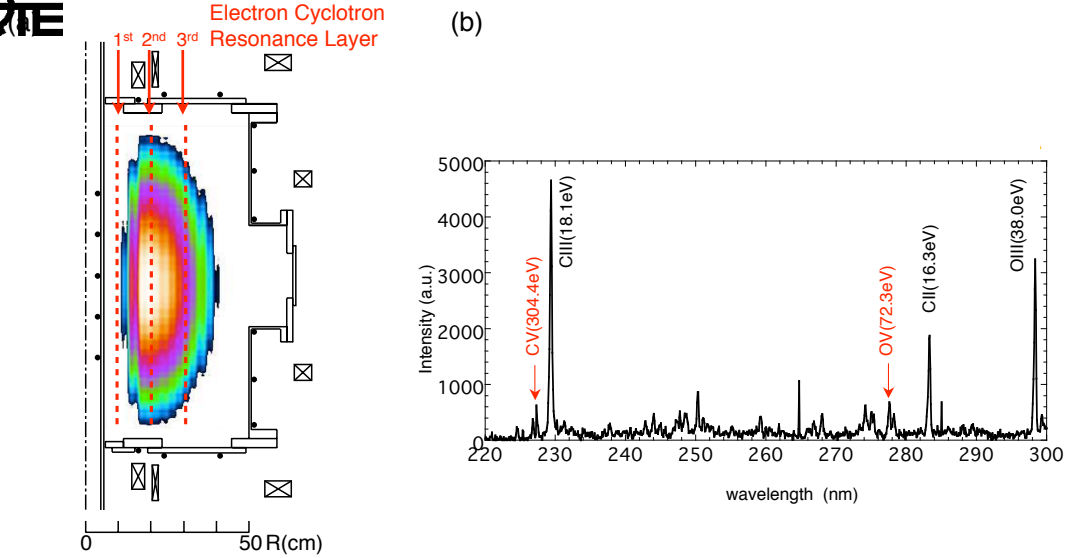


FIG. 3. (a) Soft X-ray emission profile reconstructed by CT at  $I_p = 8$  kA. (b) Impurity line spectrum at  $I_p = 5.8$  kA.

EC harmonic resonances and supports the plasma. Figure 3 (b) shows the impurity line spectrum. Impurity line radiation at relatively high excitation energies (OV(72 eV) and CV(304 eV)) are observed. The bulk electron temperature measured by a Langmuir probe for a plasma at  $I_p \sim 0.5$  kA by a microwave power of 5 kW is found to be already over 30 eV [4], where no OV nor CV lines are observed. Although no conclusive measurement has not been made on the bulk electron temperature in the plasmas at larger current level by higher microwave power injection, where insertion of a Langmuir probe into the plasma is impossible, such line radiations suggest that the bulk electron temperature increases significantly as  $I_p$  increases.

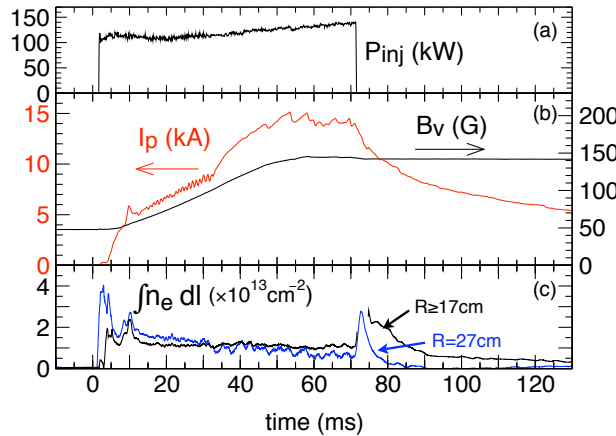


FIG. 4. Waveforms for a  $I_p = 15$  kA discharge with 5 GHz microwave. (a) Injected microwave power, (b) Plasma current and applied vertical field at  $R = 25$  cm, (c) Line-integrated electron density.

Plasma current increases much faster when the ramp-up rate of  $B_v$  is increased. Figure 4 shows the discharge where  $I_p$  increases up to 15 kA. Injected microwave power is from 100 to 130 kW. The value of  $I_p$  amounts to 16.7 % of the total toroidal coil current  $I_T$ . (Sudden

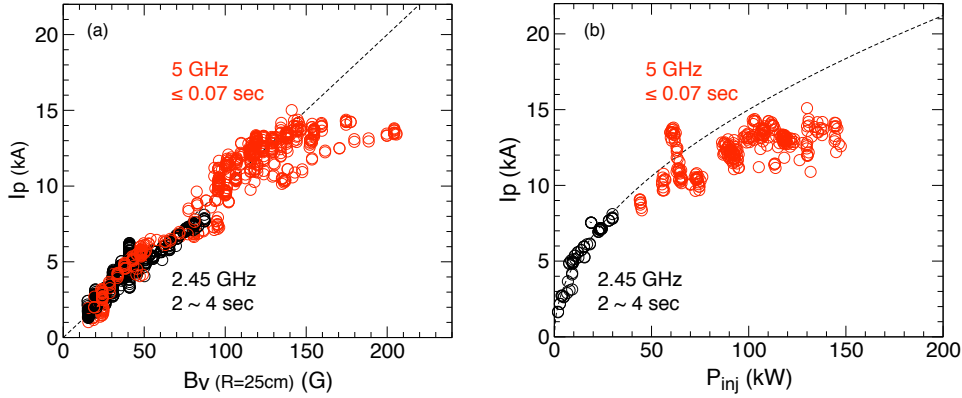


FIG. 5. Maximum plasma current as a function of (a) applied vertical field at  $R = 25$  cm, and (b) injected microwave power. Black circles are with 2.45 GHz microwave and red ones with 5 GHz microwave.

decrease and sawtooth-like wave form around 14 ~ 15 kA may be due to insufficient wall conditioning or insufficient position control.) The ramp-up rate of applied  $B_v$  is  $\sim 20$  G/10ms and the time-averaged ramp-up rate of  $I_p$  is  $\sim 2.5$  kA/10ms. In Figure 5, the maximum plasma current obtained during a pulse is plotted versus applied  $B_v$  and injected power  $P_{inj}$ . Black circles are data with 2.45 GHz microwave and red ones are with 5 GHz microwave. The maximum plasma current increases linearly with applied  $B_v$ , following the tokamak equilibrium. The temporal evolution during a pulse is also on the same line. The maximum plasma current increases also as  $P_{inj}$  but seems to scale nearly as square root of  $P_{inj}$  within present data. Some data points exceeds this scaling, where  $B_v$  is strong and plasmas are shrink to the high field side. More experimental investigation and optimisation of operation may be necessary before obtaining any conclusions.

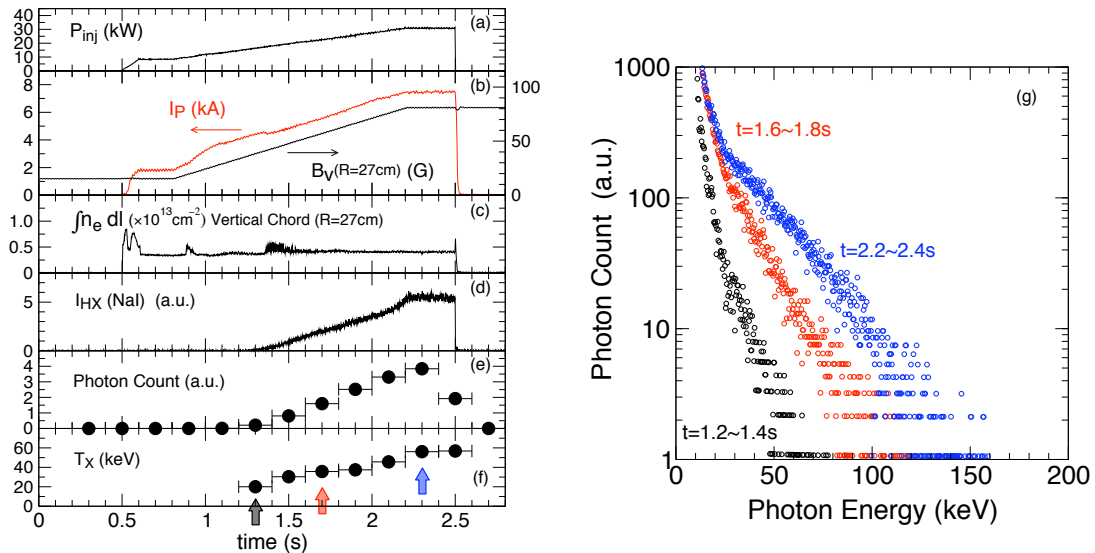


FIG. 6. Waveforms and results of X-ray pulse height analysis for discharges with 2.45 GHz microwave. (a) Injected microwave power, (b) Plasma current and applied vertical field at  $R = 27$  cm, (c) Line-integrated electron density, (d) Hard X-ray signal from NaI scintillator, (e) Photon count, (f) Tail electron temperature calculated from the slope of X-ray energy spectra, (g) X-ray energy spectra at  $t = 1.2 \sim 1.4$  s,  $1.6 \sim 1.8$  s and  $2.2 \sim 2.4$  s.

Temporal evolution of hard X-ray energy spectra is obtained in 2.45 GHz microwave discharges by the pulse height analysis with a CdTe detector. By taking advantage of the long discharge time (2 sec), it is obtained with 2 shots. As shown in Figure 6, high energy tail electrons are produced and build up during the current ramp-up and at the final stage their maximum energy reaches  $\sim 100$  keV. Coincidentally, a hot spot appears on one edge side of the limiter inserted from the outboard side. The glowing side is just that high energy tail electrons carrying the plasma current would hit on (Fig. 7). These facts suggest that a uni-directional high energy electron tail carrying plasma current is developed by EC heating.

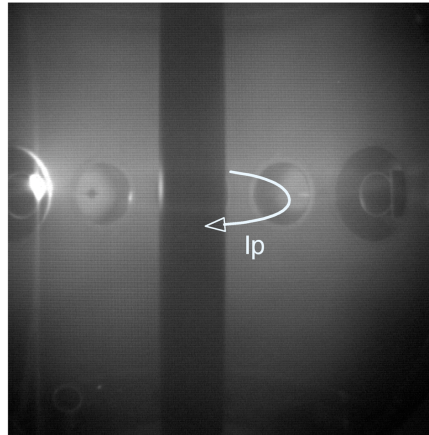


FIG. 7. A CCD image showing a hot spot on one edge side of the limiter.

The mode conversion rate from left-hand circularly polarized wave to EBW is calculated as a function of density scale length normalized by wavelength in free space by using the cold plasma resonance absorption model for LATE parameters (Fig. 8) [6]. It is shown that the mode conversion rate for 5 GHz microwave is  $\sim 80$  %, while that for 2.45 GHz microwave is  $\sim 60$  % when the density scale length  $L_n$  is  $\sim 2.4$  cm. Figure 9 shows the calculation result of EBW propagation and power absorption for 2.45 GHz microwave in the case that bulk electron temperature is 100 eV and tail electron temperatures perpendicular and parallel to magnetic field are 5 keV and 10 keV, respectively. Tail electron density is set such that total plasma current of 8 kA is carried by the tail electrons. Power absorption profile by tail electrons is broad due to Doppler effects on EC resonance condition, while that by bulk electrons is localized near the harmonic resonance layer. The amount of absorbed power by tail electrons is  $\sim 1/3$ . Then, it is expected that about 20 % of injected power is absorbed by tail electrons in total. Heat flux to the limiter is measured to estimate the loss of tail electrons. Figure 10 shows the experimental result with 2.45 GHz microwave. Power flow to the limiter is 2.4 kW, which is  $\sim 20$  % of injected power. Power flow by bulk electrons is estimated from bulk electron temperature and density measured around the limiter position by Langmuir probes and is found to be negligible small. Then the power flow to the limiter should be due to the direct loss of tail electrons and it is concluded that  $\sim 20$  % of injected power is absorbed by tail electrons. This experimental result coincides with the calculation result. Though the calculation model is simple and heat flux measurement is obtained only at the limiter, it is likely that the mode-converted EBW is absorbed by tail electrons, which carry the plasma current and are lost to the limiter.

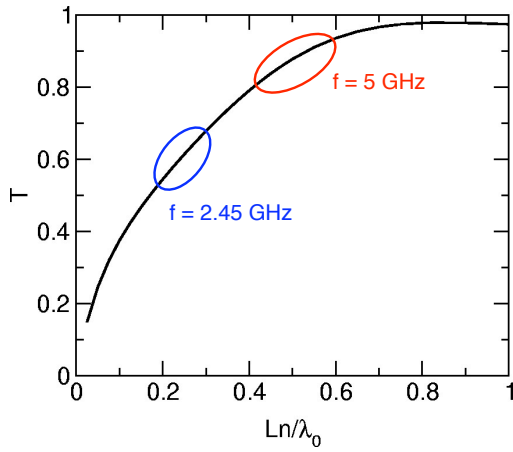


FIG. 8. The mode conversion rate from left-hand circularly polarized wave to EBW for  $\beta = \Omega e/\omega = 0.4$ ,  $N_{//} = N_{//opt} = \beta / (1 + \beta) = 0.535$  at plasma cutoff.

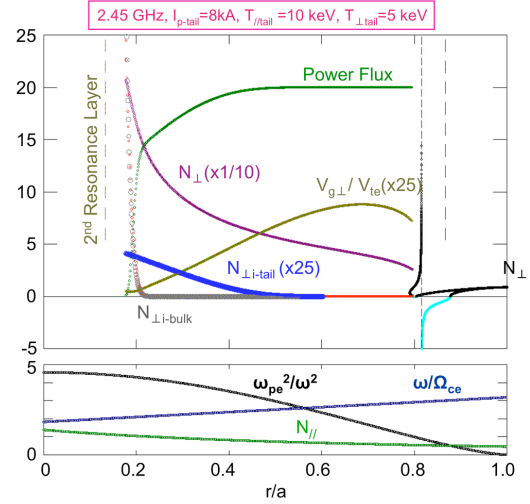


FIG. 9. EBW propagation and power absorption with a model profile of LATE parameters with 2.45 GHz microwave.

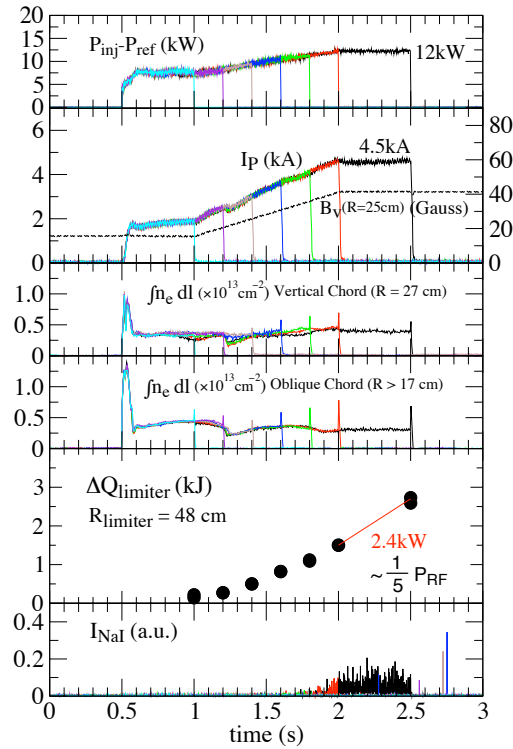


FIG. 10. Measurement of heat flow to the limiter. Power flow is obtained by changing the microwave pulse length and taking the slope of heat flow.

It is known that momentum input from EC waves with large refractive indices along the magnetic field  $N_{//}$  (say,  $N_{//} \sim 0.7$ ) becomes comparable with that from the LH waves and the ECCD efficiency approaches the LHCD efficiency for relativistic electrons [7]. And plasma current was ramped up by EC wave in WT-3 up to 6.3 kA with 2nd harmonic EC heating [8]. In a similar way, EBW with high  $N_{//}$  possess ability to diffuse resonant electrons forwardly

along field lines in velocity space, and may provide the forward force. So, in the LATE experiments, it is inferred that a uni-directional high energy electron tail is developed as plasma current increases and plasma current is ramped up by EBW-ECCD with high  $N//$ .

## 5. Summary

Spontaneous formation of initial closed flux surface occurs through a rapid current increase when a microwave is injected under a weak steady  $B_v$  and at low gas pressure. After this current jump,  $I_p$  increases by increasing  $B_v$  for equilibrium at larger plasma current. By injecting a 5GHz, 130 kW, 70 ms microwave pulse, plasma current is ramped up to 15 kA without assistance of central solenoid. It amounts to 16.7 % of the total toroidal coil current and a microwave spherical torus is produced. The electric field at the current center is negative due to self-induction during the plasma current ramp. X-ray pulse height analysis shows the presence of high energy tail electrons with energy up to  $\sim 100$  keV. Plasma current may be carried by a uni-directional high energy electron tail, which may be generated and supported by the electron Bernstein wave heating with high  $N//$ .

## References

- [1] Peng, Y.-K. M., Neumeyer, C. A., Fogarty, P. J., et al., Proc. 20<sup>th</sup> IAEA Fusion Energy Conf., IAEA-CN-116/FT/3-1Rb, Vilamoura, Portugal, 2004.
- [2] Nishio, S., Tobita, K., Tokimatsu, K., et al., *ibid.*, IAEA-CN-116/FT/P7-35.
- [3] Maekawa, T., Tanaka, H., Uchida, M., et al., Nucl. Fusion **45** (2005) 1439.
- [4] Yoshinaga, T., Uchida, M., Tanaka, H., Maekawa, T. Phys. Rev. Lett. **96** (2006) 125005.
- [5] Yoshinaga, T., Uchida, M., Tanaka, H., Maekawa, T., submitted to Nucl. Fusion.
- [6] Igami, H., Uchida, M., Tanaka, H., Maekawa, T., Plasma Phys. Control. Fusion **46** (2004) 261.
- [7] Maekawa, T., Maehara, T., Minami, T., et al., Phys. Rev. Lett. **70** (1993) 2561.
- [8] Tanaka, S., Hanada, K., Minami, T., et al, Nucl. Fusion **33** (1993) 505.